Convective heat transfer CFD analysis of forced flow through a half-stadium serpentine mini-channel at low Reynolds number

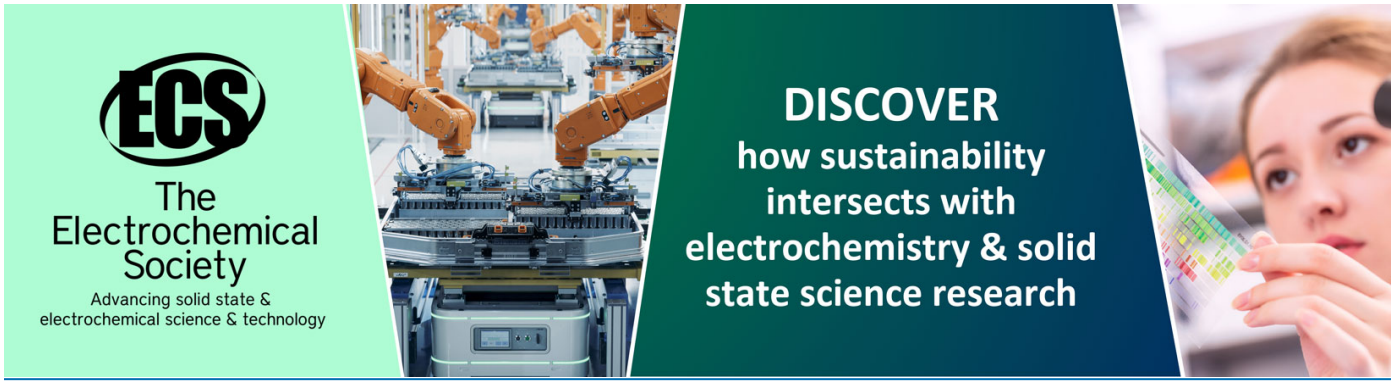

Convective heat transfer CFD analysis of forced flow through a half-stadium serpentine mini-channel at low Reynolds number

M CORTI[1], C LA TERRA[1,2], C FANCIULLI[2] and A NIRO[3]

[1,3] Politecnico di Milano, Department of Energy,
Via Lambruschini 4, 20156 Milano, Italy
[2] CNR – ICMATE, Via Previati 1/E, 23900 Lecco, Italy

[3] Corresponding author e-mail: alfonso.niro@polimi.it

Abstract. Spiral and serpentine channels are a very interesting solution to enhance heat transfer in small or miniaturized heat exchangers. In order to properly design these devices, of course, it is essential having a good knowledge of heat transfer characteristics of forced flow through this kind of ducts. However, the data base in open literature is rather lacking being investigations concerning flow mainly restricted to Dean number less than 500 and specific geometric parameters. In order to overcome these limits, a CFD analysis of a laminar forced flow through serpentine mini-channels has been started using a commercial code at finite volumes, namely Ansys Fluent. In this paper, after discussing the preliminary CFD analysis carried out on a straight pipe to tune the tool, we present the results on a flow through a half-stadium serpentine mini-channel with Reynolds number ranging between 200 and 2000. As thermal boundary conditions, a uniform wall temperature is assumed on the flat wall of the half-stadium duct, whereas the others are adiabatic. Finally, simultaneously developing flow condition is adopted. Heat transfer performances and pressure drops have been compared with ones in the straight tube, with the same length and hydraulic diameter as the serpentine duct. The results show heat transfer capability increases due to the presence of curvature as well as an earlier transition from laminar to turbulent flow.

Key Words: *forced convection, curved ducts, serpentine, mini-channels*

1. Introduction

Heat transfer enhancement is mainly driven by the need of saving energy as well as of making heat exchangers more efficient or with more compact size. This paper presents a CFD analysis of a laminar forced flow through serpentine mini-channels (Figure 1) applied in a miniaturized thermoelectric generator (TEG) [1]. Among various developments of this technology there is the will to make these TEGs portable. The size reduction involves the reduction of the surfaces designed for heat transfer, therefore arises the need to find geometries that allow to optimize the overall dimensions and, at the same time, allow an adequate heat transfer. A solution can be found using curved mini-channels, in fact the presence of the curvature plays an important role in increasing heat transfer [2].

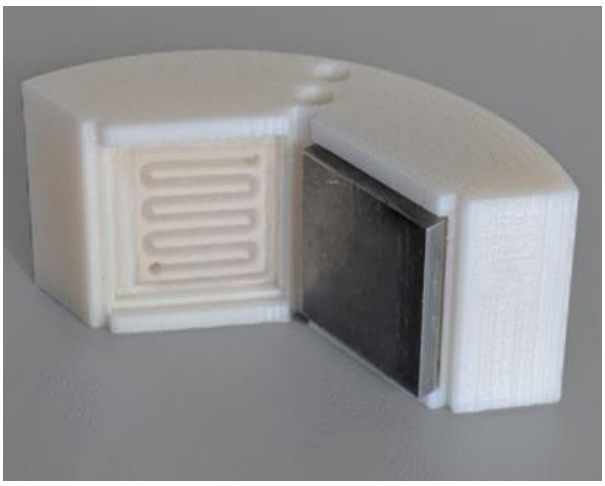

Figure 1: Serpentine mini-channels applied in TEG

As is known in literature [2], when a fluid enters a curved tube, it is pushed from the centre towards the walls of the duct due to centrifugal forces as a results of the presence of the curvature itself. The fluid consequently creates a pair of secondary flows, commonly known as Dean vortices [3]. It is thanks to the presence of these secondary flows, which promote the mixing of the fluid between the bulk region and the layers close to the walls, that an increase in the heat transfer is obtained even in laminar flows. However, the fluid motion in the curved ducts causes, in addition to an increase in heat transfer, an increase in pressure drops. It is necessary to evaluate an acceptable compromise between these two factors.

Curved channels have been studied for a long time in literature regarding classical geometries such as helical coiled tubes, sinusoidal serpentine tubes, Archimedean spirals, twisted tubes etc. but they can also be miniaturized for in-plane applications [4] and assume various shapes for which there are however no generic correlation in literature. Correlations are linked to strict constraints both geometric and related to the working fluid, and range of applicability [5], [6].

Given our field of application with Dean numbers $De = Re\sqrt{D/2R_c}$ between about 200 and 2000, there are no suitable correlations literature. Therefore, a numerical model has been developed to conduct this characterization.

2. Problem Configuration and Setup

Numerical simulations have been carried out using the software Ansys Fluent based on finite volume method. This allowed an accurate reproduction of the studied geometry as can be seen in Figure 2.

The solution domain is a 3D serpentine with a half-stadium cross section, it has been analysed with Re ranging between 200 and 2000. The working fluid is water, incompressible, with constant specific heat being far from the boiling point.

As the value of the critical Reynolds number in the present work is not known a priori, emerged the need for a mesh suitable for the study of both laminar and turbulent flow, that could capture the characteristics in both flow regimes.

The mesh created is a butterfly grid, it is a structured grid in which are simultaneously applied a Cartesian grid in the centre of the duct and a cylindrical O-grid, i.e. axial symmetric, close to the wall, around the Cartesian. Its effectiveness for modelling fluid motion within circular cross section ducts has been demonstrated in the literature [7]–[9] and this mesh has been adapted to suite an half-stadium section (Figure 3). This mesh ensures a y^+ equal to 1 at the wall to solve the laminar sublayer. To obtain a grid independent solution has been carried out a sensitivity analysis, choosing a grid with $1.6 * 10^6$ elements.

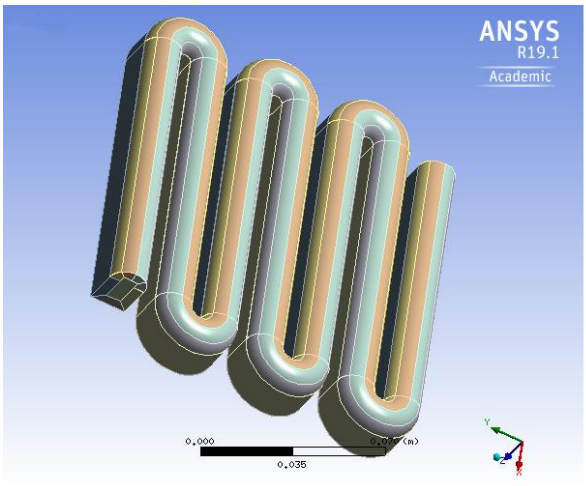

Figure 2: Serpentine mini-channel domain

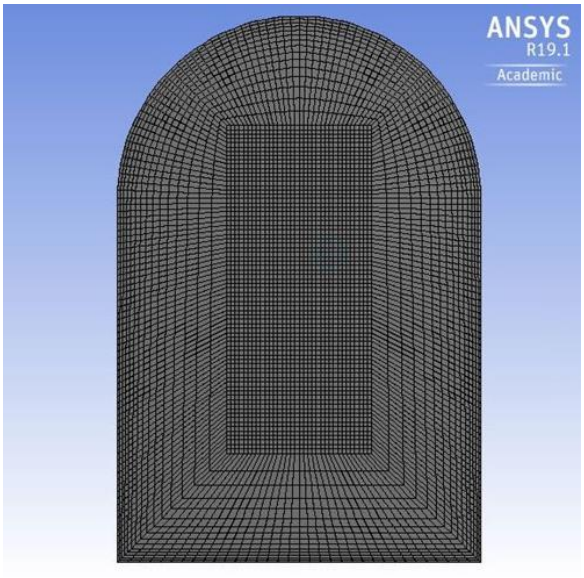

Figure 3: Adapted Butterfly grid for half-stadium cross section serpentine

The adopted mesh has the following quality parameters (Table 1).

	Element Quality	*Aspect Ratio*	*Orthogonal Quality*	*Skewness*
Mean value	0.810	0.980	0.949	0.166

Table 1: Mesh quality parameters for half-stadium cross section serpentine

2.1. Boundary Conditions

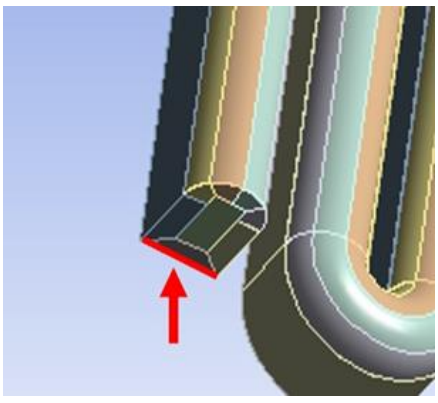

Figure 4: Heated wall at constant temperature

Inlet: mass flow inlet basing on the selected Reynolds number (for half-stadium cross section), $\dot{m} = f(Re)$. The working fluid, water, enters the channel at uniform temperature, $T_{in} = 293.15\ K$.

Outlet: pressure outlet $P_{out} = 0$ Pa .

Wall: no-slip velocity condition is applied for all the walls, moreover one wall (Figure 4) is heated at constant temperature, imposing $T_{wall} = 323.15\ K$, the other walls are diabatic, imposing $\dot{q} = 0\ W/m^2$.

2.2. Solver setting and models

The Coupled algorithm is used for pressure-velocity coupling in the case of simulations with laminar flow, while the Semi-Implicit Method for Pressure Linked Equation (SIMPLE) algorithm is used for simulations with turbulent flow.

Laminar flow has been solved with the laminar viscous model proposed by Fluent, while for turbulent flow the k-ω-SST model has been chosen between RANS turbulence models. It uses as default the Enhanced Wall Treatment (a wall function for the near-wall region i.e., viscous sublayer, buffer region and fully-turbulent outer region) [11].

Using from 15 to 30 cores Intel(R) Xeon(R) Gold 6148 CPU @ 2.40GHz, computational time has been of few hours per calculation.

Simulations stop at the level-out point in case of laminar model and at the round-off point (residuals lower than 10^{-6}) for RANS.

2.3. Preliminary CFD analysis

A preliminary CFD analysis on a straight pipe has been carried out to tune the tool.

For a straight pipe with circular cross section, the local Nusselt numbers for not fully developed laminar flow for all Reynolds analysed in the study have been numerically calculated and these values have been compared with the Nusselt numbers obtained through the Graetz problem at $Pr = \infty$ [12].

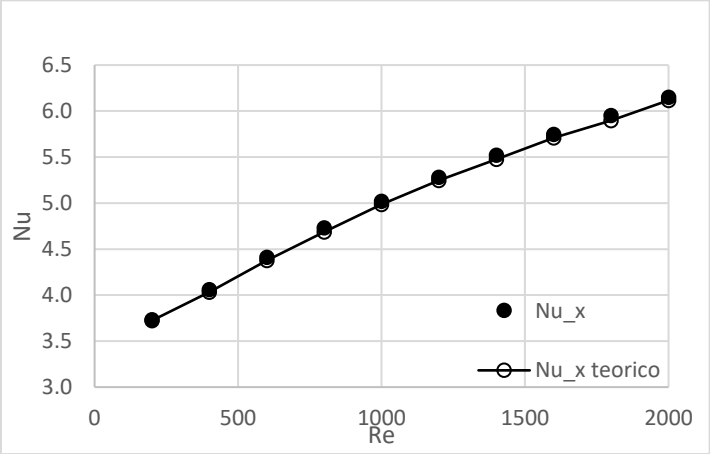

Figure 5: Local Nusselt number comparison for straight tube

The errors remained within 1% as can be seen in Figure 5. A similar procedure has been also followed in the case of a laminar fully developed flow, obtaining good agreement with the expected theoretical results.

Regarding the comparison of the average Nusselt numbers in laminar flow regime, the average Nusselt calculated through the numerical simulation has been compared with the Nusselt number calculated with the Shah-Hausen correlation [12] showing errors between 5 and 10%. Finally, a simulation for turbulent flow has been carried out and the errors on the Nusselt number resulted between 1 and 10%.

The friction factors $f_0 = (\Delta P_0/\rho)(D/L)(2/u^2)$ have been also compared with the theoretical values, obtained from the pressure drops deriving from the simulations. For laminar flow the errors remained within 1% basing on Darcy correlation [13] while for turbulent flow the errors resulted within 10% basing both on Blasius correlation and Kakac-Shah [14]. The only suitable correlation founded in literature for pressure drop for geometries similar to ours is for a circular section serpentine [15], the errors with respect to our results (for a circular section serpentine too) have been lower than 10%.

3. Results

Using Fluent the bulk temperature T_b and the heat flux q have been calculated as mean section variables, from which can be calculated the local convective heat transfer coefficient $h_x = q_x/(T_w - T_b)$ and the related Nusselt number at any section $Nu = h_x D/k$.

3.1. Earlier transition from laminar to turbulent

Regarding Nusselt number from the outlet section, the Figure 6 show $Log(Nu)$ vs $Log(Re)$ for every Reynolds number analysed.

At a certain Reynolds number, i.e. 1000, the values are more dispersed with respect to the previous ones. This lead to assume a transition in the flow regime. Another evidence was given by velocity and temperature profiles at the outlet sections too, at Re 1000 they change trend compared to the previous ones.

For Reynolds numbers affected by this phenomenon, the simulations have then been carried out according to the turbulence model k-ω-SST.

By plotting the new values of the Nusselt number in the previous graph, these points align themselves along a line with an angular coefficient different from the one of the line that interpolates only the Nusselt number calculated from laminar simulations (Figure 7).

A transition in the flow regime is confirmed, passing from laminar to turbulent around Re 1000.

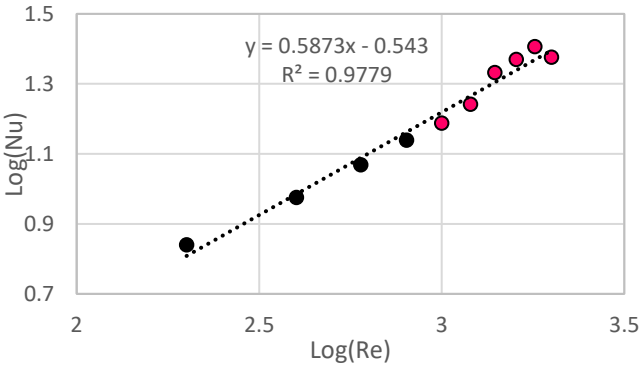

Figure 7: Nusselt numbers calculated from laminar simulation

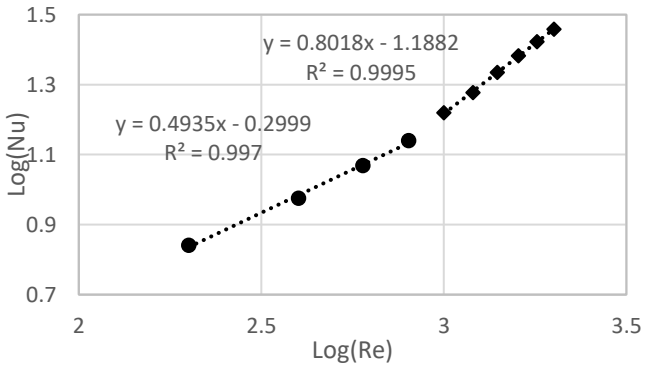

Figure 7: Nusselt numbers calculated with laminar (Re 200 - 800) and with k-ω-SST (Re 1000 - 2000)

3.2. Convective Heat Transfer Coefficient

For Reynolds number equal to 2000 the Figure 8 shows the temperature contour (taken on a plane close to the heated wall) of the fluid. It is clearly higher in the straight ducts and lower in the curved ducts of the serpentine: this implies a lower heat transfer coefficient for the straight ducts and a higher heat transfer coefficient for the curved ones. Some sections have been built along the entire coil to extract the local heat transfer coefficient (Figure 9).

Plotting the values of the local heat transfer coefficient calculated at any sections of the serpentine as a function of the length of the duct, it is visible the presence of a trend of peaks and troughs (Figure 10). In presence of curvatures the heat transfer is greater while in the straight duct parts it is lower.

Furthermore, as regards the first straight duct, away from the curvature, the value of its local convective heat transfer coefficient is lower compared to the value assumed in the subsequent straight sections as it has not yet been affected by the effects of the curvature.

This highlights that the curvature improves heat transfer.

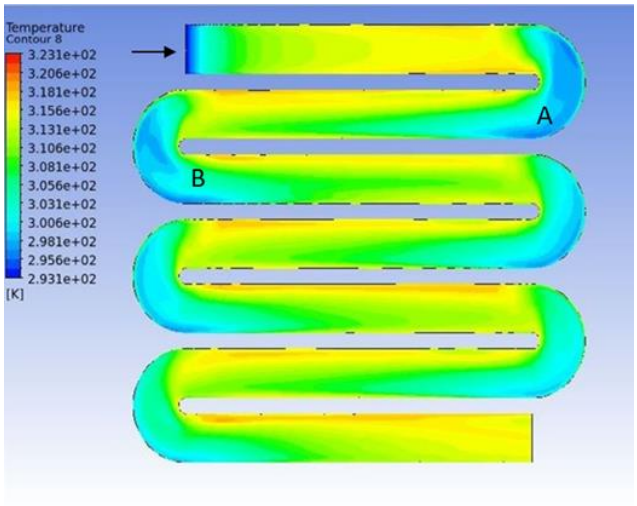

Figure 9: Temperature Contour

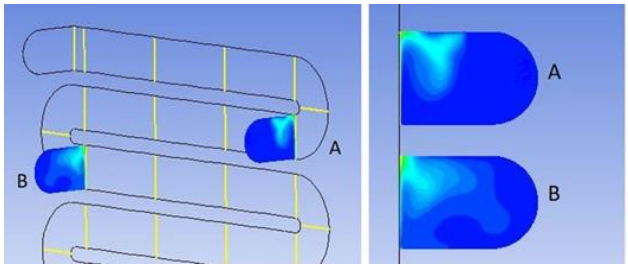

Figure 8: Sections and temperature contour

Given the fluctuating trend of the local convective heat transfer coefficient, an attempt has been made to provide a trend starting from the quantities of temperature and heat flux.

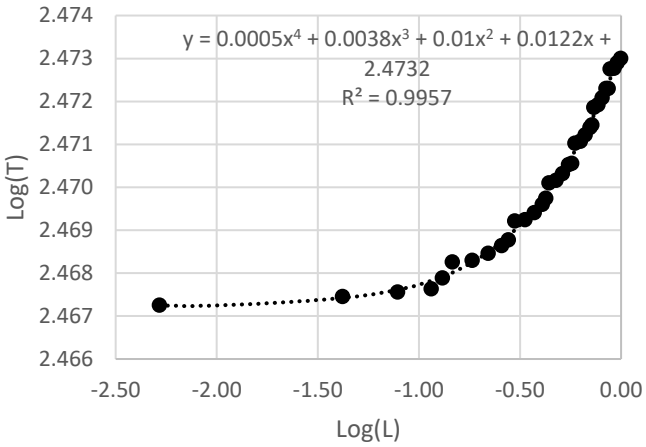

Figure 11: Local Temperature distribution

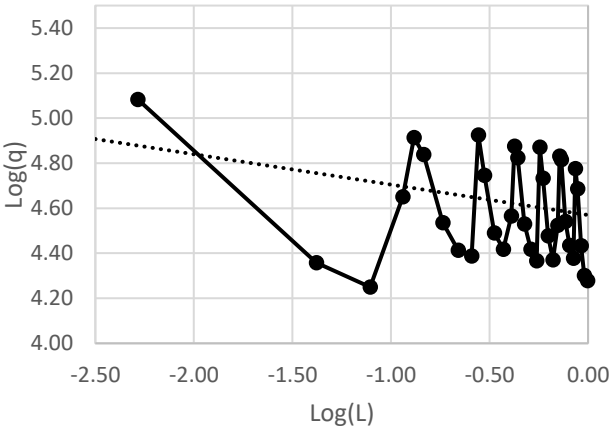

Figure 11: Local Wall Heat Flux distribution

The temperature distribution (Figure 11) in a Log-Log graph has been interpolated with a degree 4 polynomial law so as to maximize the coefficient of determination R^2.

The heat flux (Figure 12) assumes a non-monotonous trend due to the presence of curvatures; it cannot be interpolated with a polynomial function, therefore a linear interpolation has been used, albeit with a low coefficient of determination in order to provide an average trend.

By calculating the bulk temperatures and the heat flux using the trend provided, the interpolated convective heat transfer coefficient is calculated. Plotting this quantity in function of the length of the duct, a regular average trend has been obtained (Figure 10), gradually asymptotic as the x coordinate of the graph increases.

The condition of fully developed flow is reached in the duct.

Obviously it could not be possible to insert a straight duct in the TEG instead of the serpentine, but the values of the local convective heat transfer coefficient of a straight duct of same length as serpentine, same diameter and boundary conditions have been plotted in the graph (Figure 10). The local convective heat transfer coefficient of the straight tube is always smaller than the one of the serpentine.

Using the serpentine is achieved an advantage both in geometric and thermal terms.

Furthermore, by calculating the average convective heat transfer coefficient section by section and plotting the data series obtained (Figure 10), it can be seen how the values of the average convective heat transfer coefficient tend to overlap those of the local convective heat transfer coefficient deriving from the trend.

The average convective heat transfer coefficient has been computed as follows:

$$\bar{h} = \frac{1}{\sum \Delta A_x}\left(\sum_{x=1}^{n_{sez}} h_x * \Delta A_x\right)$$

As approximations, the local convective heat transfer coefficient interpolated at the outlet can be used as an estimation of the average convective heat transfer coefficient of the duct.

4. Conclusion

In conclusion, the curvature increases the heat transfer and anticipates the transition from the laminar to turbulent flow regime. Using curved mini-channels is possible to optimize heat transfer following the need of reducing size.

The serpentine mini-channel is an adequate solution for the cooling of the TEG, without affecting the electronic device.

The local convective heat transfer coefficient interpolated at the outlet of the serpentine mini-channel can be used as an estimation of the average convective heat transfer coefficient of the duct.

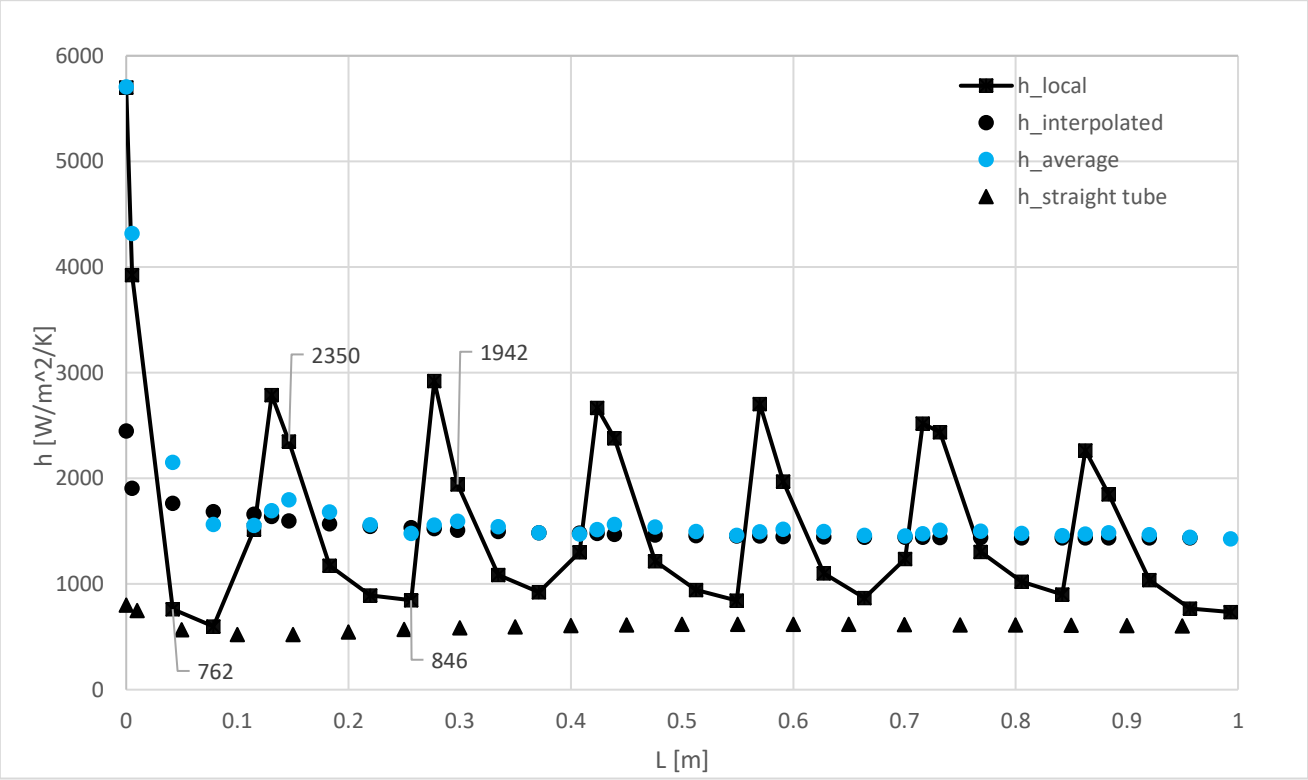

Figure 12: Local and Average Convective Heat Transfer Coefficient

Nomenclature

Symbol	Quantity	SI Unit	Symbol	Quantity	SI Unit
D	Equivalent Diameter	m	Rc	Curvature Radius	m
De	Dean Number	-	Re	Reynolds number	-
f	Friction factor	-	T_b	Bulk temperature	K
h	Convective heat transfer coefficient	W/m^2K	T_w	Wall temperature	K
k	Thermal conductivity	W/m/K	u	Bulk velocity (average)	m/s
$\dot{m}$	Mass flow rate	kg/s	y+	Dimensionless wall distance $y^+ = \Delta_{y_P}/v\sqrt{\tau_w/\rho}$	-
Nu	Nusselt number	-	τ_w	Wall shear stress	Pa
P	Pressure	Pa	ρ	Density	kg/m^3
$\dot{q}$	Wall heat flux	W/m^2	ν	Kinematic viscosity	m^2/s

References

[1] C. Fanciulli, H. Abedi, L. Merotto, R. Dondè, S. De Iuliis, and F. Passaretti, "Portable thermoelectric power generation based on catalytic combustor for low power electronic equipment," *Appl. Energy*, vol. 215, no. February, pp. 300–308, 2018.
[2] M. Ghobadi and Y. S. Muzychka, "A Review of Heat Transfer and Pressure Drop Correlations for Laminar Flow in Curved Circular Ducts," *Heat Transf. Eng.*, vol. 37, no. 10, pp. 815–839, 2016.
[3] W. R. Dean, "The stream-line motion of fluid in a curved pipe," *Philos. Mag.*, vol. 5, no. 7, pp. 208–223, 1928.
[4] P. Poredoš, U. Tomc, N. Petelin, B. Vidrih, U. Flisar, and A. Kitanovski, "Numerical and experimental investigation of the energy and exergy performance of solar thermal, photovoltaic and photovoltaic-thermal modules based on roll-bond heat exchangers," *Energy Convers. Manag.*, vol. 210, no. October 2019, p. 112674, 2020.
[5] P. L. Spedding, E. Benard, and G. M. McNally, "Fluid flow through 90 degree bends," *Dev. Chem. Eng. Miner. Process.*, vol. 12, no. 1–2, pp. 107–128, 2004.
[6] P. Naphon and S. Wongwises, "A review of flow and heat transfer characteristics in curved tubes," *Renew. Sustain. Energy Rev.*, vol. 10, no. 5, pp. 463–490, 2006.
[7] V. Hernandez-Perez, M. Abdulkadir, and B. J. Azzopardi, "Grid generation issues in the CFD modelling of two-phase flow in a pipe," *J. Comput. Multiph. Flows*, vol. 3, no. 1, pp. 13–26, 2011.
[8] V. Hernandez-Perez, "Gas-liquid two-phase flow in inclined pipes.," University of Nottingham, 2008.
[9] M. Colombo, A. Cammi, G. R. Guédon, F. Inzoli, and M. E. Ricotti, "CFD study of an air-water flow inside helically coiled pipes," *Prog. Nucl. Energy*, vol. 85, pp. 462–472, 2015.
[10] S. V Patankar and D. B. Spalding, "A calculation procedure for heat, mass and momentum transfer in three-dimensional parabolic flows," *Int. J. Heat Mass Transf.*, vol. I, pp. 1787–1806, 1972.
[11] I. ANSYS, *ANSYS Meshing User's Guide*. ANSYS, Inc., 2013.
[12] T. L. Bergman, A. S. Lavine, F. P. Incropera, and D. . Dewitt, *Fundamentals of Heat and Mass Transfer*. John Wiley & Sons, 2011.
[13] F. M. White, *Viscous Fluid Flow*. McGraw-Hill, 2006.
[14] S. Kakac, R. K. Shah, and W. Aung, *Handbook of Single-Phase Convective Heat Transfer*. John Wiley & Sons, 1987.
[15] M. Ciofalo and M. Di Liberto, "Fully developed laminar flow and heat transfer in serpentine pipes," *Int. J. Therm. Sci.*, vol. 96, pp. 248–266, 2015.